Journal of Applied Electrochemistry (2018) 48:1255–1264
https://doi.org/10.1007/s10800-018-1247-6

RESEARCH ARTICLE

A five-fold efficiency enhancement in dye sensitized solar cells fabricated with $AlCl_3$ treated, SnO_2 nanoparticle/nanofibre/nanoparticle triple layered photoanode

G. K. R. Senadeera[1,2,3] · A. M. J. S. Weerasinghe[1,3] · M. A. K. L. Dissanayake[1,3] · C. A. Thotawatthage[1,2]

Received: 26 April 2018 / Accepted: 6 August 2018 / Published online: 13 August 2018
© Springer Nature B.V. 2018

Abstract

The use of electrospun nanofibre (NF) membrane of SnO_2 toward the efficiency enhancement in dye sensitized solar cells (DSSCs) with a triple layered, $AlCl_3$ treated SnO_2-based photoanode is presented. The performance of DSSCs fabricated with SnO_2 nanoparticle (NP)-based photoanode is compared with that of DSSCs made with a novel triple layered SnO_2 photoanode of configuration FTO/NP/NF/NP. Thickness of the NF membrane is optimized to achieve the highest solar cell performance. Solar cells made with single layer SnO_2 NP photoanode sensitized either by Eosin-Y dye or Indoline dye showed efficiencies of 0.3% and 2.02%, respectively, under the irradiance of 100 mW cm^{-2} (AM 1.5), while the corresponding devices with $AlCl_3$-treated, triple layered photoanode showed efficiencies of 1.55 and 2.77%, respectively, under the same illumination. Accordingly, more than five-fold enhancement in overall efficiency is achieved in DSSCs by using this novel SnO_2-based photoanode with the optimized thickness of the SnO_2 nanofibre membrane and sensitized with Eosin-Y dye. Scanning electron microscopic studies revealed that the SnO_2 nanofibre membrane consists of an interconnected network-like structure formed by the SnO_2 nanofibres. Electrochemical impedance spectroscopy measurements on DSSCs made with these two types of photoanodes reveals that the series resistance of the DSSC made with the novel NP/NF/NP triple layered photoanode is significantly reduced. The observed higher electron lifetime determined from Bode plots shows that electron recombination is lower in the DSSCs made with the triple layered photoanode. Improved light harvesting by multiple scattering effects within the triple layered photoanode structure and the suppression of the electron recombination by Al_2O_3 sub-nanometer-sized coating around SnO_2 appear to be the major factors for the enhancement in photo current density and efficiency.

Graphicasl Abstract

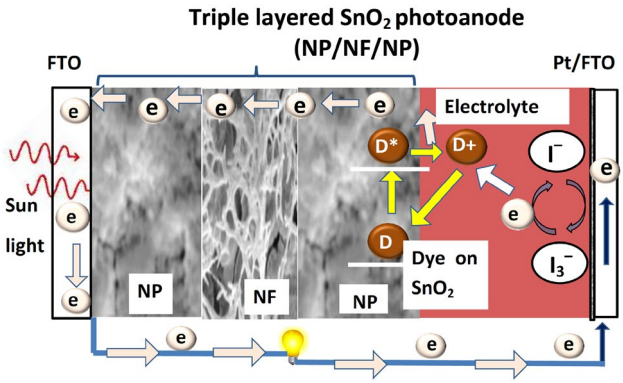

Keywords Electro-spun SnO_2 nano nanofibres · Triple-layered photoanode · Dye-sensitized solar cells · Eosin-Y · Indoline · $AlCl_3$ treatment

Extended author information available on the last page of the article

1 Introduction

Dye sensitized solar cells (DSSCs) can be considered among the most promising alternatives for the conventional silicon-based solar cells [1–4]. Typically, a DSSC consists of a dye-sensitized wide band gap semiconducting photoanode such as TiO_2, an electrolyte and a platinum-coated counter electrode. In these devices, under illumination and upon excitation of the dye molecules, the photo-generated electrons are transferred to the conduction band of a wide band gap semiconductor. Redox mediator in the electrolyte regenerates the dye cations receiving electrons from the external circuit via the counter electrode [1, 2]. Photo-conversion efficiencies greater than 12% are reported for these solar cells with the use of the TiO_2 photoanodes sensitized with ruthenium dye [3, 4]. Morphology and the electrical properties of the photoanode are some of the crucial factors in determining the overall efficiencies of these devices. Since the amount of dye adsorbed to the surface of the semiconductor determines the generation of photocurrent, generally the photoanodes are fabricated with nanoparticles having high specific surface area and also with sizable and optimized thickness [5–9]. However, due to poor adherence of the semiconductor material to the conducting glass substrate where it is deposited, and the poor light transmittance through the semiconductor, the thickness of the photoanode cannot be increased beyond a certain limit. Increase of the photoanode film thickness beyond this optimized value increases the grain boundary effects that negatively affect the efficient electron transfer [2, 8]. Therefore, numerous techniques such as the use of nano particles (NP) [3–8], one dimensional nanowires (NW) [9, 10], nanofibres (NF) [11–15] and nanotubes (NT) [16, 17] and nanorods (NR) [18, 19] etc. of TiO_2 have been used successfully toward achieving higher conversion efficiencies in these devices. Apart from the TiO_2, other metal oxides such as SnO_2, ZnO, and Nb_2O_5 and are also used as photoanodes in DSSCs due to their desired properties such as easy preparation techniques and low cost [20]. Among these, SnO_2 is also a wide band gap, n-type semiconductor ($E_g \sim 3.6$ eV at 300 K) with high electron mobility (100–250 $cm^2\ V^{-1}\ s^{-1}$) [21, 22]. Hence, it is used in a broad range of applications such as solar cells, gas sensors, optoelectronic devices, batteries, and antireflective coatings [23–27]. However, the use of SnO_2 as a photoanode in DSSCs is not so popular due to the low power conversion efficiencies. Sandeep et al. have reported that the influence of the thickness of SnO_2-based photoanode on the performance of Eosin-Y dye-sensitized solar cells [28]. According to these authors, the highest efficiency of 0.55% has been achieved by employing a 8 μm thick SnO_2-based photoanode and further increase of the thickness of the semiconductor has decreased the overall efficiency of the devices. Alternatively, many researchers have attempted to enhance the efficiencies of SnO_2 photoanode-based solar cells using different nanostructured morphologies like nanotubes, nanoflakes, nanofibres, and nanotubes of SnO_2 [29–32]. Preparing composites of SnO_2 with other semiconductors like ZnO and TiO_2 or treating with $AlCl_3$ or the use of core–shell structures of SnO_2 with nano size insulating layers are the most commonly used methods to improve the efficiencies of these solar cells [33, 34]. Despite the use of composites of SnO_2 with other semiconductors or the modification of the mohopology of the material, the efficiency enhancement in DSSCs can also be achieved by increasing the light harvesting by using nanostructurally modified multi-layered photoanodes. This can be achieved by using a double layered structure in which the second layer comprises of bigger size particles [35, 36]. For TiO_2 photoanode-based DSSCs, it has been established that it is not possible to achieve higher efficiencies merely by increasing the thickness of the single layer TiO_2 photoanode due to the formation of cracks and poor adherence of the thicker semiconductor film to the conducting glass substrate [8, 15]. In this context, as an alternative approach, recent work by our group on DSSCs based on TiO_2-based photoanodes has shown that the efficiency of DSSCs can be substantially increased by replacing the widely used single TiO_2 NP layer-based photoanode with a triple layered composite photoanode structure of configuration NP/NF/NP [15, 37, 38]. Here, the efficiency enhancement is achieved due to the increase in light absorption by multiple scattering effects within the tri-layered photoanode structure. Due to the previously mentioned favorable physical properties and low cost of SnO_2, it is of interest to develop DSSCs based on nanostructurally configured SnO_2 photoanodes. However, to the best of our knowledge, the use of a scattering layer of nanofibres (NF) of SnO_2 in a triple layered NP/NF/NP photoanode structure toward the efficiency enhancement in DSSCs has not been reported so far. In order to demonstrate this tri-layer effect in the present work, we have used two metal free organic dyes, Eosin, and Indoline as sensitizers.

As it is well established, recombination of the electrons generated by the dye molecules in the DSSCs can be suppressed by introducing a thin insulating layer of a material such as Al_2O_3 or MgO around nanoparticles of the wide band gap semiconducting material resulting a significant enhancement of the overall efficiency of the device [25, 26]. Therefore, in this study, we have used the $AlCl_3$ treatment in the fabrication of SnO_2 composite, triple layered photoanode, which after sintering, is expected to form a thin sub nanometer size coating of Al_2O_3 around SnO_2 nano particles and nanofibres thereby inhibiting the electron–hole recombination by passivation of surface states through which recombination can occur otherwise [25].

2 Experimental

2.1 Preparation of SnO_2 nano particle (NP) layer

In order to compare the performance of DSSCs, comprising single layer NP and the novel three layered photoanode, two kinds of photoanodes having the same thicknesses were fabricated on fluorine doped tin oxide (FTO) coated glass substrate with the configurations FTO/NP and FTO/NP/NF/NP. At first, a NP layer of SnO_2 was deposited on FTO glass substrates Nippon sheet glass, sheet resistance 10–12 ohms per square (Ω/□) by a spraying technique with a normal air compressor. Precursor solution for spraying was prepared as follows. 2 ml of colloidal aqueous SnO_2 solution (Alfa Aesar 15% in H_2O) and 2.5 ml of acetic acid (Sigma Aldrich 99.8%) were first mixed and ground in an agate mortar. 100 ml of ethanol was added to the mixture and sonicated for 10 min. and sprayed at a constant pressure and a flow speed on to FTO glass substrates which were kept at 150 °C. Thickness of the NP layer was varied by varying the time duration of spraying of the precursor solution. Films were then sintered at 550 °C for 45 min. Some of the SnO_2 photoanodes were then immersed in 1 mM $AlCl_3$ (BDH 99%) for 24 h and gently washed with ethanol and dried using a hot air flow. Subsequently, the anodes with and without $AlCl_3$ treatment were immersed separately in 0.1 mM ethanolic dye solutions of either Eosin Y (BDH) or Indoline (DATO, China) for dye adsorption. Current–voltage characteristics were measured for DSSCs fabricated with photoanodes of different thicknesses which were assumed to be proportional to the spraying time of the precursor solution. From these measurements, the optimum thickness of the SnO_2 NP film which corresponds to the best solar cell was identified and determined using scanning electron microscopy (SEM).

2.2 Preparation of SnO_2 nanofibres (NF) and triple layered photoanode structure

SnO_2 nanofibres were prepared by using an electrospinning system (Nabond Technologies, Hong Kong). The precursor solution for electro spinning was prepared by mixing 0.8 g of $SnCl_2{:}2H_2O$ (Riedel-deHaën 98%) with dimethylformamide (DMF) and ethanol (BDH 99.96%). The solution was magnetically stirred for 2 h and then 1.45 g of poly(vinyl acetate) (Aldrich, M_w:140,000) was added. The solution was again magnetically stirred overnight to obtain a clear solution to ensure that all the $SnCl_2{:}2H_2O$ powder was completely dissolved. In the electrospinning system, 13 kV DC voltage was applied between the spinneret and the drum collector. The distance between the tip and the drum collector was kept at 8 cm and the syringe pump flow rate was maintained at 0.6 ml h^{-1}. These are the parameters optimized to get uniform SnO_2 nanofiber membranes. In order to obtain the FTO/NP/NF structure, the FTO substrate with previously prepared $AlCl_3$-treated SnO_2 NP film having the optimized amount of NPs prior to dye adsorption, were fixed to the drum collector of the electrospiner and precursor solution was then electrospun to obtain a NF membrane of SnO_2 making the FTO/NP/NF structure. During this process, rotating speed of the drum was kept at 630 rpm. In order to change the thickness of the nanofibre membrane, different electrospinnig times were used with the same precursor solution. Photoanodes with FTO/NP/NF configuration were then sintered at 550 °C for 45 min. Finally, another NP layer of SnO_2 was sprayed on this FTO/NP/NF structure by the spray method described previously to obtain the triple layered FTO/NP/NF/NP SnO_2-based photoanode nanostructure which was subsequently sintered at 550 °C for 45 min. Subsequently, dye adsorption of these photoanodes was done as described earlier and fabrication and testing of DSSCs were carried out by the method mentioned in Sect. 2.3.

2.3 Fabrication of DSSCs and current–voltage measurements

A liquid electrolyte consisting of 0.5 M tetrapropyl ammonium iodide (Aldrich 98%) (0.738 g) and 0.03 M I_2 (Fluka 99.8%) (0.060 g) in a mixture of acetonitrile (BDH) (1.0 ml) and ethylene carbonate (Fluka 99%) (3.6 ml) was used to fabricate the DSSCs. At first the mixture of above chemicals except iodine was magnetically stirred until the solutes were fully dissolved and then appropriate amount of iodine was added and the mixture was stirred for another 12 h in a closed bottle. DSSCs of configurations FTO/NP/electrolyte/Pt-FTO and FTO/NP/NF/NP/electrolyte/Pt-FTO were fabricated with two different photoanodes described above by placing the electrolyte between the photoanode and a Pt-coated FTO counter electrode. A schematic diagram of the solar cell fabricated with the triple layered SnO_2-based photoanode structure is shown in Fig. 1. The thicknesses of the two different SnO_2-based photoanodes, FTO/NP and FTO/NP/NF/NP used in this work were kept the same in order to ensure that there is no effect on the photoelectric performance of DSSCs from the anode thickness variation. The current–voltage (*I–V*) characteristics of the DSSCs were measured under the illumination of 100 mW cm^{-2} using a Xenon 500 lamp with a AM 1.5 filter with a homemade computer-controlled setup coupled to a Keithley 2000 multimeter and a potentiostat/galvanostat HA-30.

2.4 Electrochemical impedance spectroscopy (EIS) measurements

Electrochemical impedance spectroscopic (EIS) measurements of DSSCs fabricated with above two SnO_2-based

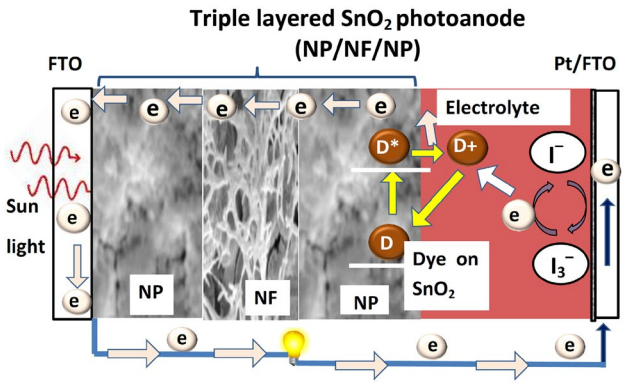

Fig. 1 Schematic diagram showing the DSSCs fabricated with triple layered SnO_2 photoanode

photoanodes were measured under the illumination of 100 mW cm^{-2} using a Potentiostat/Galvanostat (Metrohm Autolab PGSTAT 128N) in the frequency range from 0.1 Hz to 100 kHz. Bode plots were obtained from the EIS data.

3 Results and discussion

3.1 Current–voltage characteristics of DSSCs

Figure 2 shows the efficiencies of the Indoline dye sensitized solar cells fabricated with different SnO_2-based $AlCl_3$-treated photoanode thicknesses. Since the amount of material deposited on the substrate and hence the thickness of the NP film increase with the volume of the precursor solution sprayed and the time duration of spraying, the scaling in the *x*-axis of the figure was taken to be proportional

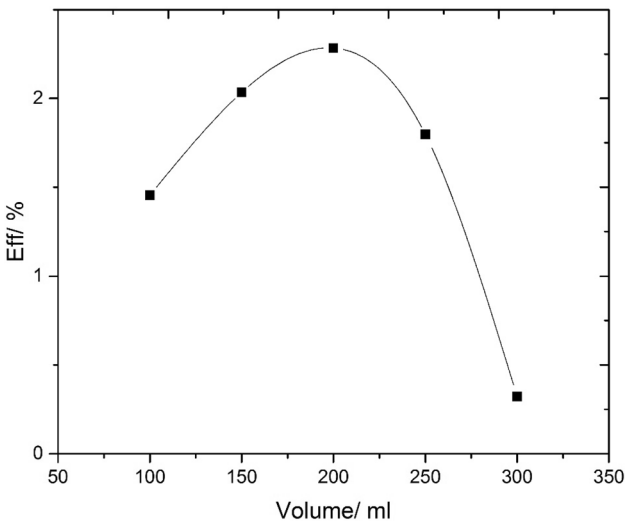

Fig. 2 Efficiency variation of the DSSCs with the volume of tin oxide precursor solution

to the thickness of the SnO_2 film. As it is evident from the figure, DSSC made with the photoanode prepared by spraying of 200 ml of precursor solution has given the highest efficiency of 2.28%. Beyond this optimum thickness of the photoanode, the efficiency of DSSC decreases with increasing film thickness of the photoanode. Corresponding *I–V* data such as short circuit current density (J_{sc}), open circuit voltage (V_{oc}), fill factor (FF), and the efficiency (η %) of all these DSSCs are tabulated in Table 1 with respect to their sprayed amount of the precursor solution. When the thickness of the SnO_2 film increases, the effective total surface area available for dye adsorption also increases. Because of this, the generation of photoelectrons and hence, the photocurrent also increases resulting an increase in the efficiency [1, 2]. However, as it is observed and reported by others, when the thickness of the photoanode is increased further beyond the optimum value, even though the amount of dye adsorption increases, the overall film resistance and the rate of electron recombination also increase. As a result, the photocurrent and the efficiency decreases after reaching the optimum film thickness. Similar trends have also been reported by Wang et al. [35] and Sandeep et al. [28]. Based on these observations, SnO_2 NP photoanodes prepared by spraying 200 ml of precursor solution exhibiting best solar cell performance was used for further studies.

In order to identify the optimum thickness of the SnO_2 NF membrane, SnO_2 NF membranes of different thicknesses were electrospun on the aforementioned SnO_2 NP layer (on FTO/NP). This was done by varying the elctrospinning time from 1 to 10 min. After sintering the FTO/SnO_2(NP)/SnO_2(NF) composite structure, a third layer of SnO_2 nanoparticles (NP) was applied on the top of the above NF layer as mentioned in the previous section in order to obtain the triple layered SnO_2 photoanode with configuration FTO/NP/NF/NP having different NF membrane thicknesses (assumed to be proportional to different electrospinning times). Here, it should be noted that, in order to maintain the consistency and the constant thickness of the NP layer, the volume of precursor solution and the spraying condition and also the time duration was kept unchanged. Therefore, we believe that the thicknesses of the NP layer fabricated in all the

Table 1 Photovoltaic parameters of DSSCs with the configuration of FTO/NP/electrolyte/Pt-FTO, fabricated with different amounts of SnO_2 precursor solution

Spray volume (ml)	J_{SC} (mA cm^{-2})	V_{oc} (mV)	FF (%)	η (%)
100	8.252	397.2	44.4	1.46
150	7.800	453.3	57.5	2.03
200	8.916	443.7	57.8	2.28
250	6.304	459.8	62.0	1.80
300	4.032	170.2	46.9	0.32

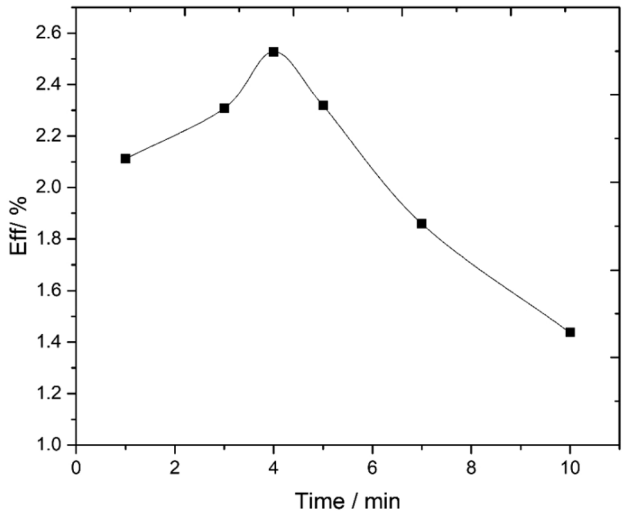

Fig. 3 Efficiency variation of the DSSCs with the SnO_2 nanofibre electrospun time (assumed to be proportional to film thickness)

instances under the same conditions are the same. Prior to fabricating the solar cells, both types of SnO_2 photoanodes (FTO/NP and FTO/NP/NF/NP) were subjected to $AlCl_3$ treatment as previously described. DSSCs were fabricated using the same electrolyte described under Sect. 2.3. Figure 3 shows the efficiency variation of DSSCs vs. the electrospun time of the precursor solution. Since the electrospinning conditions used in the fabrication of NF membranes such as the applied voltage, the distance between the tip and the collector, flow rate, concentration and the viscosity of the precursor solution are fixed, it can be assumed that the thickness of the NF membrane would be uniform and constant throughout this fabrication and proportional to the electrospinning time only.

As can be seen from the figure, the efficiency of DSSCs first increases with the electrospun time. The highest efficiency was obtained with 4.0 min duration and a sharp decrease in the efficiency was observed for elctrospun times longer than this. Therefore, in this study, the SnO_2 NF layer prepared with 4.0 min electrospun time was selected for further studies. The actual thickness of the cross section of the tri-layered phtoanode with NF membrane showing the best DSSC performance was measured using the SEM.

Figure 4 shows the current–voltage (*I–V*) characteristics of the DSSCs fabricated with different SnO_2 photanodes sensitized with either Inodoiline dye (Fig. 4a) or Eosin-Y dye (Fig. 4b). As it was observed by our group in one of the previous studies [25], in order to further enhance the efficiencies of the DSSCs, a post treatment by $AlCl_3$ was done as described in the Experimental section before the dye adsorption of the photoanode. Solar cell parameters extracted from these figures are tabulated in Table 2.

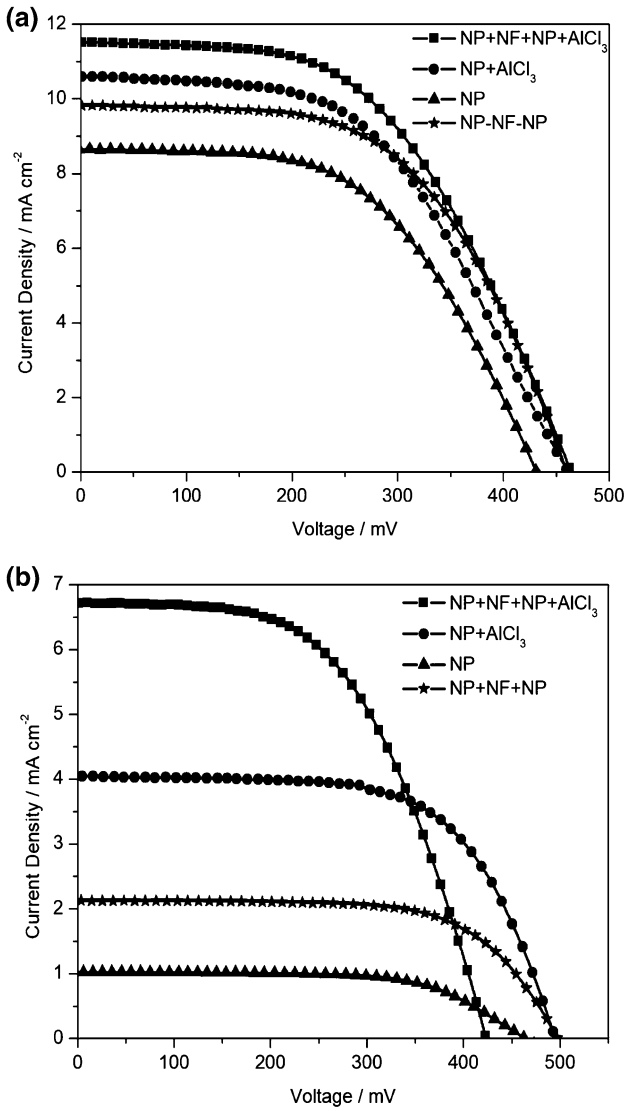

Fig. 4 a Photocurrent density vs. photovoltage (*J–V*) characteristics of the DSSCs with Indoline dye. **b** Photocurrent density vs. photovoltage (*J–V*) characteristics of the DSSCs with Eosin Y dye

As evident from Table 2, DSSCs fabricated only with the sprayed SnO_2 NP film show the lowest efficiency for both types of dyes. It gives the maximum efficiency of 2.02% for the Indoline dye and 0.30% for the Eyosin-Y dye. The post treatment with $AlCl_3$ has significantly enhanced the efficiencies of DSSCs for both these dyes. This is possibly due to the enhanced basicity of the Al sites binding the dye molecules strongly to the post treated SnO_2 particles with $AlCl_3$ as we have observed in our previous work [25]. Moreover, the $AlCl_3$ treatment not only facilitates the efficient dye adsorption but also suppresses the electron recombination process [25].

As shown in Table 2, the DSSCs fabricated with SnO_2 NP/NF/NP triple layer photoanodes show enhanced

Table 2 Photocurrent and voltage variation of DSSC systems fabricated with different SnO_2 photoanodes sensitized with Indoline and Eosin Y dyes

SnO_2 electrode	With indoline dye				With Eosin-Y dye			
	J_{sc} (mA cm^{-2})	V_{oc} (mV)	*FF* %	η (%)	J_{sc} (mA cm^{-2})	V_{oc} (mV)	FF (%)	η (%)
NP	8.66	432.5	53.8	2.02	1.03	464.2	63.9	0.30
NP ($AlCl_3$ treated)	8.92	443.7	57.8	2.28	2.13	494.6	63.5	1.27
NP/NF/NP	10.61	460.9	55.7	2.53	4.06	498.6	65.8	0.70
NP/NF/NP ($AlCl_3$ treated)	11.53	464.6	51.6	2.77	5.45	424.2	54.5	1.55

efficiency compared to the DSSCs made with a single layered SnO_2 NP photoanode of similar thickness. A remarkable enhancement in J_{sc} from 2.13 to 5.45 mA cm^{-2} can be seen for the Eosin–Y dye sensitized solar cell due to the triple layered photoanode effect. This is more than 100% enhancement in J_{sc}. The $AlCl_3$ treatment combined with the triple layer effect has raised the efficiency of these solar cells from 0.30 to 1.55% reflecting an overall fivefold increase in efficiency. As it is observed in both cases, incorporation of NF layer in the triple layered structure has improved the short circuit current density of the DSSCs significantly. The increase of the photocurrent in the triple layered SnO_2 photoanode appears to be due to the increased light absorption by multiple scattering events within the nanofibre structure as seen in several DSSC systems sensitized with Ru 719 dye as well as PbS:Hg quantum dot sensitized solar cells [15, 37, 38].

According to our previous findings on DSSCs fabricated with TiO_2-based NP/NF/NP triple layer photoanode, an efficiency enhancement of 32% has been achieved [15]. The corresponding efficiency enhancement of DSSCs made of SnO_2-based triple layered photoanodes used in this work for the Eosin Y dye is 133% (from 0.30% for the NP-based cells to 0.70% for the NP/NF/NP based cells). Therefore, this enhancement is much superior to the efficiency enhancement shown by corresponding TiO_2-based DSSCs due to the triple-layer effect.

3.2 SEM analysis of SnO_2 based photoanodes

The surface morphologies of SnO_2 photoanodes were examined by the SEM. Figure 5 shows the SEM photographs of the top view of sprayed NP (Fig. 5a) and as produced electrospun SnO_2 NF films (Fig. 5b). Figure 5c shows the surface morphology (top view) of a NF film after sintering. As can be seen from Fig. 4a, the spray deposited NP SnO_2 films contain aggregated and interconnected SnO_2 nanoparticles. According to Fig. 5b, prior to sintering the phtoanode with NF film, heavily branched interconnected nanofibre structure could be seen. Overlapping nanofibres may stick together (cross linking) to form this type of branched and interconnected network structure. The estimated average diameter of an individual SnO_2 nanofibre is around 200 nm. However, it can be observed that after sintering, the formation of a rigidly interconnected and highly porous SnO_2 NF structure (Fig. 5c) [36, 39–41].

Figure 5d shows a selected SEM image of the cross section obtained using the NP/NF/NP triple layered SnO_2 photoanode. According to this figure, the thickness of each NP layer is around 1.2–1.4 μm and the total thickness of the SnO_2 tri-layered photoanode is approximately 2.77 μm.

3.3 EIS analysis of SnO_2 based photoanodes

EIS measurements were used to find the interfacial recombination kinetics as well as the interfacial resistances of the DSSCs. The Nyquist plots obtained from EIS measurements of DSSCs with different photoanode structures sensitized with Eosin Y are shown in Fig. 6 (left) as a representative example. By using a suitable electrical equivalent circuit (inset Fig. 6a), the interfacial resistances were estimated using a computer software.

Series resistance (R_s), charge transfer resistance of the Pt/electrolyte interface (R_{1CT}), charge transfer resistance of the TiO_2/electrolyte interface (R_{2CT}) extracted from the equivalent circuit analysis are given in Table 3. The value of the resistance, R_s is interpreted as the overall series resistance and the effects associated with deformations in the photoanode material [15, 42]. Further, it is also influenced by the inter-particle and inter-fibre connectivity of the photoanode [41, 43].

DSSCs prepared with only SnO_2 nanoparticle phtoanode shows the highest series resistance as depicted in the table. The series resistance of the DSSCs made with novel triple layer SnO_2 photoanode structure (NP/NF/NP) is significantly lower compared to that of the DSSC made with only NP layer. This could be related to the enhanced photoelectron generation due to the improved light harvesting in the DSSCs with the triple layered structure compared to the DSSC with NP photoanode. However, R_s values of both photoanode structures (NP and NP/NF/NP) have increased possibly due to the $AlCl_3$ post treatment. This could be due to the formation of the thin barrier layer in the SnO_2 photoanode structure. On the other hand, the value of the charge

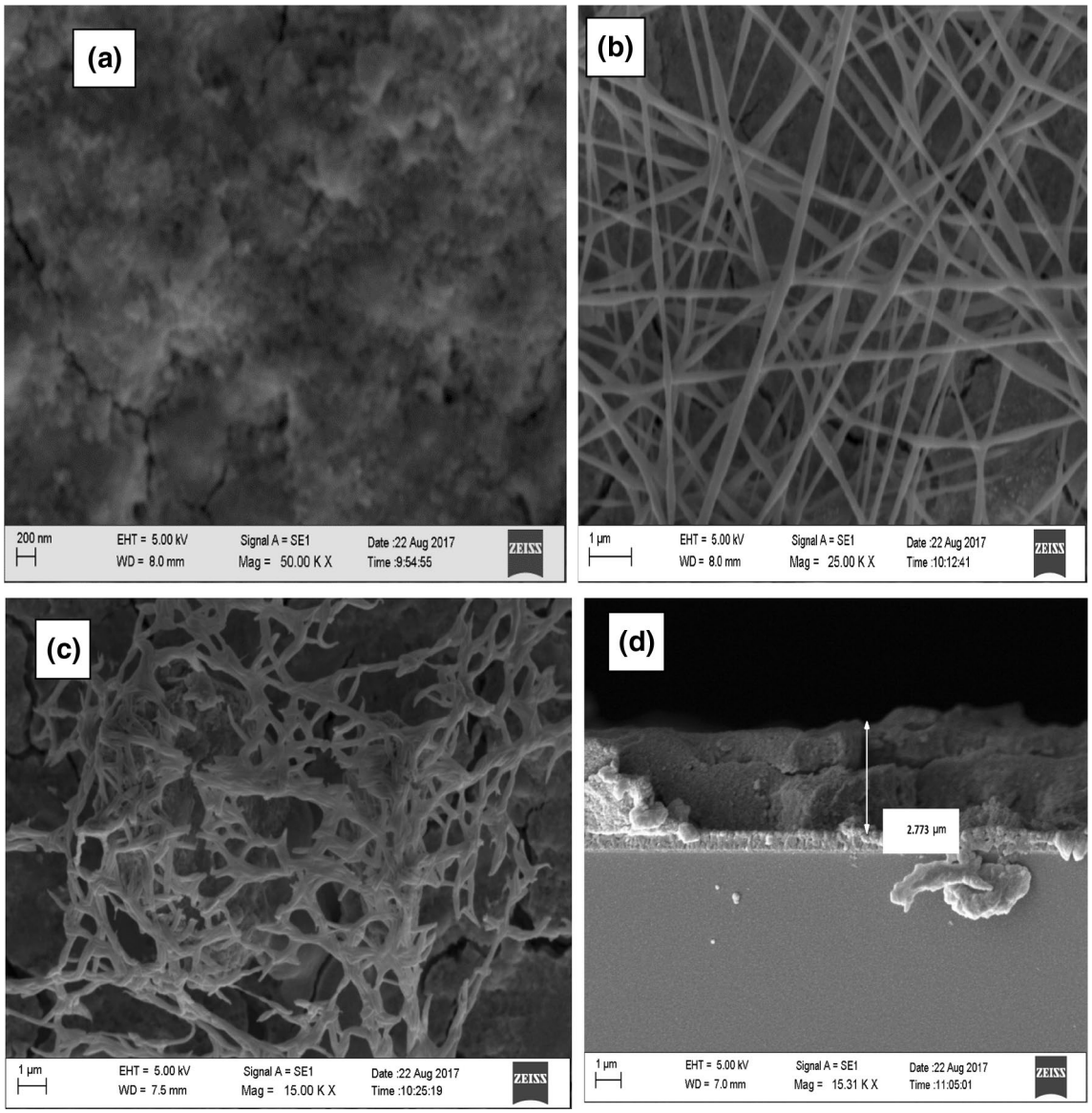

Fig. 5 SEM images of different SnO_2 films used in the photoanodes: **a** sprayed SnO_2 film, and **b** electrospun nanofibres before sintering and **c** after sintering at 550 °C and **d** cross sectional view of the triple layered photoanode

transfer resistance of the Pt/electrolyte interface (R_{1CT}) decreases with the $AlCl_3$ treatment for both types of photoanodes facilitating the efficient electron transfer in devices. However, the charge transfer resistance of the TiO_2/electrolyte interface (R_{2CT}) is higher in the triple layered structure and this could be due to the lower interfacial connectivity between the NF and NP layers in the untreated photoanode.

Figure 6b shows the Bode plots derived from the above Nyquist plots. As it is depicted in the figure, the value of the maximum angular frequencies (ω_{max}) of both NP and NP/NF/NP photoanodes are shifted toward the lower frequency side due to the AlCl3 treatment. Electron lifetimes in these devices are calculated by using the following relationship and values are tabulated in the Table 3.

$$\tau_e = \frac{1}{\omega_{\max}} = \frac{1}{2\pi f_{\max}}$$

where f_{max} is the maximum frequency of the mid-frequency peak.

According to the values in the Table 3, the electron life time in the DSSCs fabricated with $AlCl_3$-treated NF composite triple layered photoanode is greater than that of the NP photoanode. Therefore, the back electron recombination is lower in the DSSCs fabricated with the novel SnO_2 triple layered photoanode.

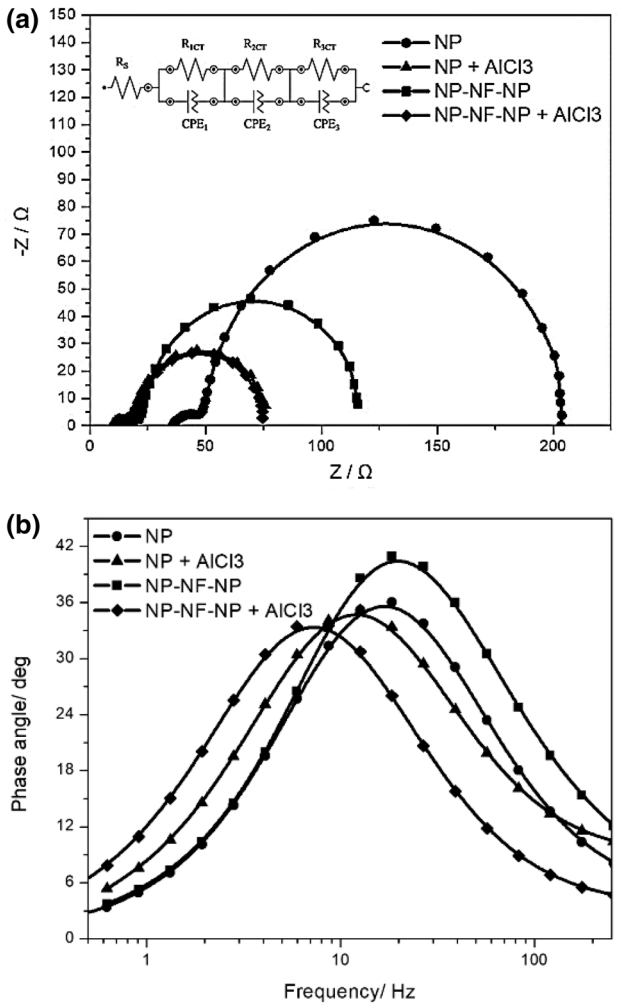

Fig. 6 **a** Nyquist plots obtained for Eosin Y based DSSCs, **b** Bode plots obtained for Eosin Y based DSSCsl

Table 3 Interfacial resistances of the Eosin Y-based DSSCs from EIS data together with Frequency peaks and electron lifetime values

Photoanode structure with Eyosin-Y dye	R_s (Ω)	R_{1CT} (Ω)	R_{2CT} (Ω)	f_{max} (Hz)	τ_e (ms)
NP	35.5	14.2	52.0	16.8	9.4
NP + $AlCl_3$	10.1	5.4	58.6	12.0	13.2
NP-NF-NP	14.0	15.6	83.8	19.9	7.9
NP-NF-NP + $AlCl_3$	13.5	2.5	56.3	7.3	21.8

4 Conclusions

In this study, we have demonstrated that a significant efficiency enhancement in SnO_2-based DSSCs can be achieved by using a novel triple layered photoanode fabricated with a SnO_2 nanofibre layer sandwiched between two SnO_2 nanoparticle layers and sensitized with Indoline and Eosin Y dyes. Further enhancement of the efficiency has been obtained with the post treatment of the photoanodes with $AlCl_3$. Remarkable overall enhancement in the photocurrent as well as a considerable enhancement in the efficiency of DSSC has been achieved by combining both, the triple layer effect and the $AlCl_3$ post treatment. Enhanced multiple light scattering by the nanofibre layer in the triple layered photoanode combined with the suppression of the back reaction by Al_2O_3 sub-nano sized coating around SnO_2 appears to be the major reason for this enhancement as reflected from the increase in the photo current density. Reduction of electron recombination due to the enhancement in the electron life time and the reduction of series resistance of the photoanode contribute to the overall enhancement in the efficiency as seen from the EIS analysis. Thus, by replacing the single layered SnO_2 photoanode with this novel triple layered photoanode along with post treatment with $AlCl_3$, more than five-fold efficiency enhancement has been obtained in the SnO_2 based DSSCs.

References

1. Oregan B, Grätzel M (1991) A low-cost, high-efficiency solar cell based on dye-sensitized colloidal TiO_2 films. Nature 353:737–740
2. Grätzel M (2000) Perspectives for dye-sensitized nanocrystalline solar cells. Prog Photovoltaics Res Appl 8:171–185
3. Gao F, Wang Y, Shi D, Zhang J, Wang M, Jing X, Humphry-Baker R,. Wang P, Zakeeruddin SM, Grätzel SM M (2008) Enhance the optical absorptivity of nanocrystalline TiO_2 film with high molar extinction coefficient ruthenium sensitizers for high performance dye-sensitized Solar cells. J Am Chem Soc 130:10720–10728
4. Mathew S, Yella A, Gao P, Humphry-Baker R, Curchod BFE, Ashari-Astani N, Tavernelli I, Rothlisberger U, Nazeeruddin MDK, Grätzel M (2014) Dye-sensitized solar cells with 13% efficiency achieved through the molecular engineering of porphyrin sensitizers. Nature Chemistry 6:242–247
5. Grätzel M (2004) Conversion of sunlight to electric power by nanocrystalline 2 dye-sensitized solar cells. J Photochem Photobiol A 164:3–14
6. Grätzel M (2003) Dye-sensitized solar cells. J Photochem Photobiol C 4:145–153
7. Wu SL, Lu HP, Yu HT, Chuang SH, Chiu CL, Lee CW, Diau EW, Yeh CY (2010) Design and characterization of porphyrin sensitizers with a push–pull framework for highly efficient dye-sensitized solar cells. Energy Environ Sci 3:949–955
8. Senadeera GKR, Kobayashi S, Kitamura T, Wada YS, Yanagida S (2005) Versatile preparation method for mesoporous TiO_2 electrodes suitable for solid-state dye sensitized photocells. Bull Mater Sci 28(6):635–641
9. Maheswari D, Sreenivasan D (2015) Review of TiO_2 nanowires in dye sensitized solar cells. Appl Sol Energy 51:112–116
10. Hailiang L, Qingjiang Y, Huang Y, Yu C, Li RZ, Wang J, Guo F, Zhang Y, Zhang X, Wang P, Zhao L (2016) Ultra-long rutile TiO_2 nanowire arrays for highly efficient dye-sensitized solar cells. ACS Appl Mater Interfaces 8(21):13384–13391

11. Li J, Chen X, Ai N, Hao J, Chen Q, Strauf S, Shi Y (2011) Silver nanoparticle doped TiO_2 nanofiber dye sensitized solar cells. Chem Phys Lett 514:141–145
12. Leung YL (2011) Application of a bilayer TiO_2 nanofiber photoanode for optimization of dye-sensitized solar cells. Adv Mater 23:4559–4562
13. Jung WH, Kwak NS, Hwang TS, Yi KB (2012) Preparation of highly porous TiO2 nanofibers for dye-sensitized solar cells (DSSCs) by electro-spinning. Appl Surf Sci 261:343–352
14. Nair AS, Shengyuan Y, Peining Z, Ramakrishna S (2010) Rice grain-shaped TiO_2 mesostructures by electrospinning for dye sensitized solar cells. Chem Commun 46:7421–7423
15. Dissanayake MAKL, Divarathna HKDWMN, Dissanayake CB, Senadeera GKR, Ekanayake PMPC, Thotawattage CA (2016) An innovative TiO_2 nanoparticle/ nanofiber/ nanoparticle, three layer composite photoanode for efficiency enhancement in dye-sensitized solar cells. J Photochem Photobiol A 322–323:110–118
16. Roy P, Albu SP, Schmuki P (2010) TiO_2 nanotubes in dye-sensitized solar cells: Higher efficiencies by well-defined tube tops. Electrochem Commun 12:7:949–951
17. Kim GS, Seo HK, Godble V, Kim YS, Yang OB, Shin HS (2006) Electrophoretic deposition of titanate nanotubes from commercial titania nanoparticles: application to dye-sensitized solar cells. Electrochem Commun 8:961–966
18. Kathirvel S, Su C, Shiao YJ, Lin YF, Chen BR, Li WR (2016) Solvothermal synthesis of TiO_2 nanorods to enhance photovoltaic performance of dye-sensitized solar cells. Sol Energy 132:310–320
19. Jeng MJ, Wung YL, Chang LB, Chow L, (20130, Dye-sensitized solar cells with anatase TiO2 nanorods prepared by hydrothermal method. Int J Photoenergy. https://doi.org/10.1155/2013/280253
20. Liu X, Fang J, Liu Y, Lin T (2016) Progress in nanostructured photoanodes for dye-sensitized solar cells. Front Mater Sci 10(3):225–237
21. Birkel A, Lee YG, Koll D, Meerbeek XV, Frank SF, Choi MJ, Kang YS, Char K, Tremel W (2012) Highly efficient and stable dye-sensitized solar cells based on SnO2 nanocrystals prepared by microwave-assisted synthesis. Energy Environ Sci 5:5392–5396
22. Soumen Das S, Jayaraman V (2014) SnO_2: a comprehensive review on structures and gas sensors. Prog Mater Sci 66:112–255
23. Pan S, Li G (2011) Recent progress in p-type doping and optical properties of SNO_2 nanostructures for optoelectronic device applications. Recent Pat Nanotechnol 5:138–161
24. Tennakone K, Kumara GRA, Kottegoda IRM, Perera VPS (1999) An efficient dye-sensitized photoelectrochemical solar cell made from oxides of tin and zinc. Chem Commun 1:15–16
25. Perera VPS, Senadeera GKR, Tennakone K (2003) Sensitization of aluminum chloride adsorbed tin (IV) oxide nanocrystalline films with Rose Bengal. J Colloid Interface Sci 265(2):15, 428–431
26. Tennakone K, Bandara J, Bandaranayake PKM, Kumara GRRA, Konno K, Enhanced efficiency of a dye-sensitized solar cell made from MgO-coated nanocrystalline SnO2, Jpn J Appl Phys 40: 2, 7B, L732-734
27. Snaith HJ, Ducati C (2010) SnO_2-based dye-sensitized hybrid solar cells exhibiting near unity absorbed photon-to-electron conversion efficiency. Nano Lett 10:1259–1265
28. Arote S, Prasadad MBR, Tabhane V, Pathan H (2015) Influence of geometrical thickness of SnO_2 based photoanode on the performance of Eosin-Y dye sensitized solar cell. Opt Mater 49:213–217
29. Gao C, Li X, Lu B, Chen L, Wang Y, Teng F, Wang J, Zhang Z, Pan X, Xie EA (2012) facile method to prepare SnO_2 nanotubes for use in efficient SnO2-TiO2 core-shell dye-sensitized solar cells. Nanoscale 7(11):3475–3481
30. Yi-YuBu I (2017) Light harvesting, self-assembled SnO2 nanoflakes for dye sensitized solar cell applications. Optik 147:39–42
31. Kasaudhan R, Elbohy H, Sigdel S, Qiao H, Wei Q, Qiao Q (2014) Incorporation of TiO2 nanoparticles into SnO2 nanofibers for higher efficiency dye-sensitized solar cells. IEEE Electron Device Lett 35(5):578–580, May 2014
32. Gao C, Li X, Lu B, Chen L, Wang Y, Teng F, Wang J, Zhang Z, Xiaojun P, Xie E (2012) A facile method to prepare SnO_2 nanotubes for use in efficient SnO2-TiO2 core-shell dye-sensitized solar cells. Nanoscale 4(11):3475–3481
33. Kim HW, Shim SH (2006) Study of ZnO-coated SnO_2 nanostructures synthesized by a two-step process. Appl Surf Sci 253:510–514
34. Chappel S, Chen SG, Zaban A (2002) TiO_2-coated nanoporous SnO2 electrodes for dye-sensitized solar cells. Langmuir 18(8):3336–3342
35. Wang YF, Li KN, Wu WQ, Fan Xu YF, Chen HY, Su CY, Kuang DB (2013) Fabrication of double layered photoanode consisting of SnO2 nanofibers and nanoparticles for efficient dye-sensitized solar cells RES advances 3(33):13804–13811
36. Song W, Gong Y, Tian J, Cao G, Zhao H, Sun C (2016) A novel photoanode for dye-sensitized solar cells with enhanced light harvesting and electron collection efficiency. Appl Mater Interfaces 8(21):13418–13425
37. Dissanayake MAKL, Sarangika HNM, Senadeera GKR, Divarathna HKDWMNR, Ekanayake EMPC (2017) Application of a nanostructured, tri-layer TiO2 photoanode for efficiency enhancement in quasi-solid electrolyte-based dye- sensitized solar cells. J Appl Electrochem 47:11,1239–1249
38. Dissanayake MAKL, Jaseetharan T, Seenadeera GKR, Thotawatthage CA (2018) A novel, PbS:Hg quantum dot-sensitized, highly efficient solar cell structure with triple layered TiO_2 photoanode. J Electrochim Acta 269:172–179
39. Apriani T, Arsyad WS, Wulandari P, Hidayat R (2016) Investigation on the influences of layer structure and nanoporosity of light scattering TiO_2 layer in DSSC J Phys 739(012134):1–6
40. Zhu L, Zhao YL, Lin XP, Gu XQ, Qiang YH (2014) The effect of light-scattering layer on the performance of dye-sensitized solar cell assembled using TiO_2 double-layered films as photoanodes. Superlattices Microstruct 65:152–160
41. Arote S, Rajendra Prasad MB, Tabhane V, Pathan H (2015) Influence of geometrical thickness of SnO_2 based photoanode on the performance of Eosin-Y dye sensitized solar cell. Opt Mater 49:213–217
42. Anjusree GS, Bhupathi A, Balakrishnan A, Vadukumpully S, Subramanian KRV, Sivakumar N, Ramakrishna S, Nair SV, Nair AS (2013) Fabricating fiber, rice and leaf-shaped TiO_2 by tuning the chemistry between TiO_2 and the polymer during electrospinning. RSC Adv 3:16720–16727
43. Elumalai NK, Jose R, Archana PS, Hellappan V, Ramakrishna S (2012) Charge transport through electrospun SnO_2 nanoflowers and nanofibers: role of surface trap density on electron transport dynamics. J Phys Chem C 116:22112–22120

Affiliations

G. K. R. Senadeera[1,2,3] · A. M. J. S. Weerasinghe[1,3] · M. A. K. L. Dissanayake[1,3] · C. A. Thotawatthage[1,2]

✉ M. A. K. L. Dissanayake
makldis@yahoo.com

[1] National Institute of Fundamental Studies, Hanthana Road, Kandy, Sri Lanka

[2] Department of Physics, The Open University of Sri Lanka, Nawala, Nugegoda, Sri Lanka

[3] Postgraduate Institute of Science, University of Peradeniya, Peradeniya, Sri Lanka